Supplementary information for "Magnetoelectric coupling through the spin flop transition in Ni_3TeO_6"

M. O. Yokosuk,[1] Amal al-Wahish,[1] Sergey Artyukhin,[2] K. R. O'Neal,[1] D. Mazumdar,[1] P. Chen,[1] Junjie Yang,[3] Yoon Seok Oh,[2,4] Stephen A. McGill,[5] K. Haule,[2] Sang-Wook Cheong,[2,3,4] David Vanderbilt,[2] and J. L. Musfeldt[1,6]

[1]*Department of Chemistry, University of Tennessee, Knoxville, Tennessee 37996 USA*

[2]*Department of Physics and Astronomy, Rutgers University, Piscataway, New Jersey 08854, USA*

[3]*Laboratory for Pohang Emergent Materials and Max Plank POSTECH Center for Complex Phase Materials, Pohang University of Science and Technology, Pohang 790-784, Korea*

[4]*Rutgers Center for Emergent Materials, Rutgers University, Piscataway, New Jersey 08854, USA*

[5]*National High Magnetic Field Laboratory, Florida State University, Tallahassee, Florida 32310, USA*

[6]*Department of Physics and Astronomy, University of Tennessee, Knoxville, Tennessee 37996 USA*

Assignment of the d-to-d excitations

A Tanabe-Sugano diagram provides a useful framework with which to reveal the nature of on-site d-to-d excitation in transition metal-containing materials. The diagram for a d^8 electron configuration is shown in Fig. S1(a). The strength of the crystal field is, of course, given by Dq/B. The red vertical line indicates a best fit of the crystal field strength for Ni_3TeO_6. Taking a closer look, the lowest energy excitations (at that value of Dq/B) are expected to be $^3A_2 \rightarrow {}^3T_2$, $^3A_2 \rightarrow {}^1E$, and $^3A_2 \rightarrow {}^3T_1$. Here, $^3A_2$ is the ground state. Figure S1(b) shows a close-up view of the same diagram, rotated by 90° for comparison with the measured absorption spectrum of Ni_3TeO_6. Each excitation in the absorption matches with predicted excitations from the Tanabe-Sugano diagram. This indicates that the peaks seen the absorption spectrum of Ni_3TeO_6 should be assigned as on-site d-to-d excitations. This very general framework for Ni^{2+}-containing materials is extended by our more detailed calculations (described below) which account for the subtly different environments of Ni1, Ni2, and Ni3.

Calculation details

The density of states and RPA susceptibility were calculated using the Elk code and LDA+U approximation with $U = 4$ eV on Ni d orbitals. In order to estimate the d-to-d transition energies we have used the Wien2K-DMFT code by Kristjan Haule to calculate the Wannier functions within the energy window spanning only the $3d$ Ni orbitals. The dynamic crystal field produced by oxygens in DMFT is then replaced by the static crystal field, encoded in the Wannier orbital energies. The on-site Hamiltonians (using $J_H = 0.9$ eV) in the basis of these Wannier functions were diagonalized independently for the three Ni sites and the distances

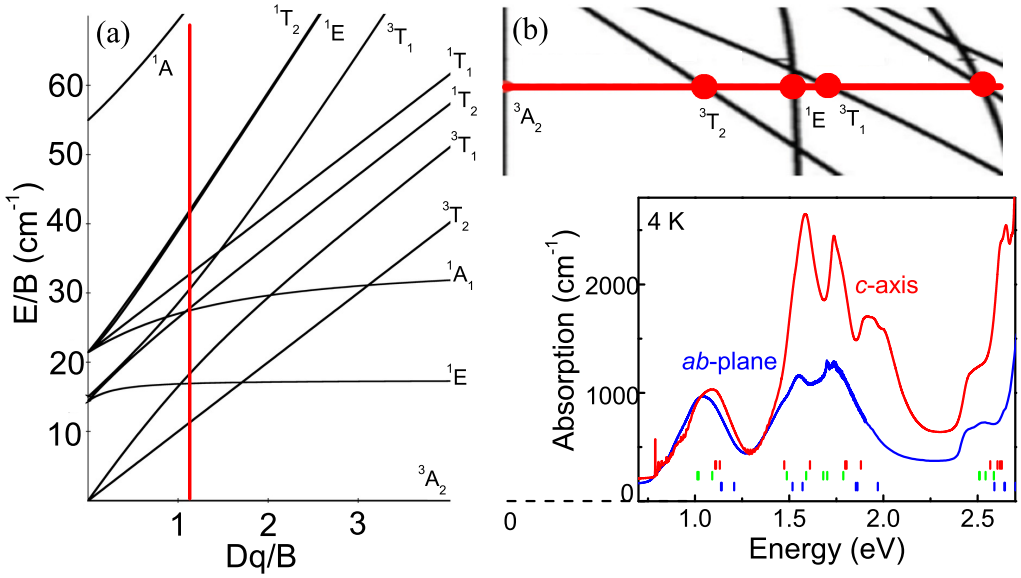

FIG. S1: (a) Tanabe-Sugano diagram for a Ni^{2+} center in the d^8 configuration. The crystal field strength of Ni_3TeO_6 is shown in red. (b) Here, the Tanabe-Sugano diagram is turned on its side and paired with the absorption spectrum along the *ab*-plane and *c*-axis. The calculated Ni *d*-to-*d* excitations for each of the three distinct Ni centers are displayed as red, green, and blue hash marks. Expectations from the Tanabe-Sugano diagram and the theoretically predicted excitations align very well with our experimental observations.

between the ground and excited states were used to approximate the *d*-to-*d* transition energies. These energies are marked by red, green, and blue vertical bands in Fig. S1(b). The calculated excitations for Ni1, Ni2, and Ni3 group into band clusters that are located in the general vicinity of the *d*-to-*d* transitions identified from the much simpler Tanabe-Sugano model discussed above.

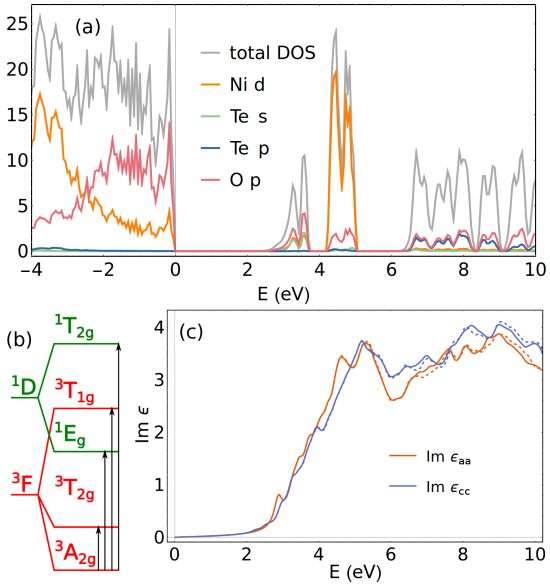

FIG. S2: (Color online) Results of DFT calculations on Ni_3TeO_6: (a) ion-projected density of states per magnetic unit cell, (b) splitting of free Ni ion d^8 multiplets in the presence of an octahedral crystal field and the crystal field excitations between these levels, and (c) components of linear optical dielectric response tensor calculated within the random phase approximation in the $q \to 0$ limit with no microscopic contributions (solid lines: with spin-orbit coupling included; dashed: without).

Temperature dependence around the magnetic transition

Along with the field induced changes across the spin flop transition, we also tested whether the electronic properties of Ni_3TeO_6 were sensitive to the 53 K magnetic ordering transition. Figure S3 shows absorption difference spectra as a function of temperature at fixed field. No distinctive changes are observed across the Neél transition. In other words, the temperature dependence in this range is very systematic.

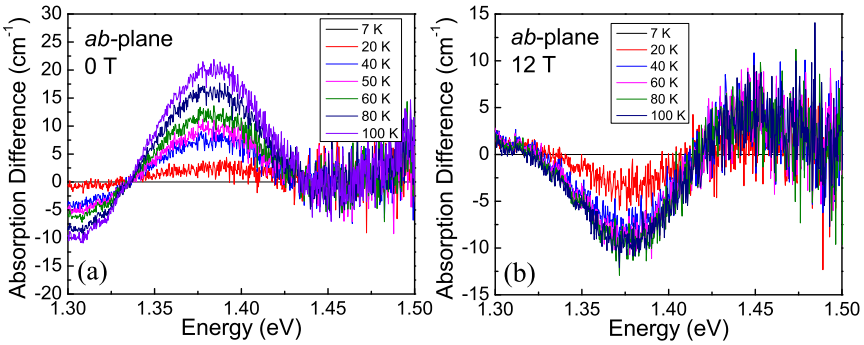

FIG. S3: Variable temperature absorption difference, $\Delta\alpha = [\alpha(E, T)$ - $\alpha(E, T = 7$ K)], at (a) 0 T and (b) 12 T.

Absolute absorptions in high magnetic field

Figure S4 shows the absorption spectra of Ni_3TeO_6 in the *ab*-plane and along *c* at 0 and 35 T. The full field data was back-calculated by adding the absorption difference curve at 35 T (calculated as $\Delta\alpha = \alpha(E, B = 35\ T) - \alpha(E, B = 0\ T)$) to the spectrum taken at 0 T. As in the main text, the absorption difference spectrum is plotted for comparison. Because the three Ni ions have different local environments (and therefore different crystal field splittings), each set of Ni *d*-to-*d* excitation energies is distinct. Since the Ni3 environment is most distorted from a perfect octahedral environment, it has the largest crystal field splitting, and the predicted excitations emanating from these sites have the overall highest energies. By contrast, the Ni2 centers have the least distortion, the smallest crystal field splitting, and the overall lowest energies within each cluster of excitations. This is equivalent to moving left and right along the Dq/B axis of Fig. S4(a).

It's easy to see from Fig. S4 that the optical properties of Ni_3TeO_6 change with applied field. A closer view is, however, required to link these modifications with distortions and the associated crystal field splittings around each of the Ni centers. For comparison, each cluster of excitations (both predicted and measured) is shown separately in Figs. S5 and S6. While some energy windows are more revealing than others, several general trends emerge.

For instance, in the majority of cases, the leading edge of the band (and sometimes other energy windows near the center) are affected by magnetic field. This suggests that the local environment around Ni2 (and probably Ni1 as well) becomes more distorted, although probably still remaining within the same point group. By contrast, the trailing edge of each of the bands has very limited or no field dependence. Since

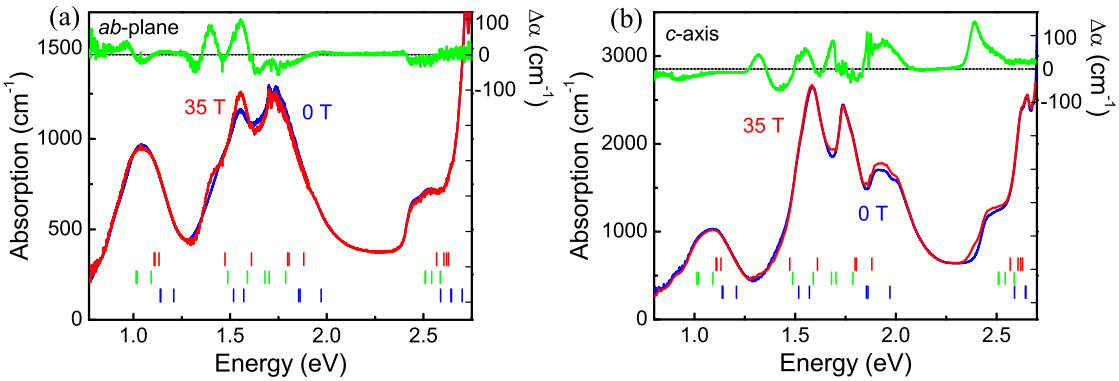

FIG. S4: (a) Absolute absorption spectrum of Ni_3TeO_6 at 0 and 35 T in the *ab*-plane along with the full field absorption difference at 4.2 K. (b) Absorption spectrum at 0 and 35 T in the *c*-direction along with the absorption difference given by $\Delta\alpha = \alpha(E, B = 35\ T) - \alpha(E, B = 0\ T)$ at 4.2 K. The vertical tick marks at the bottom of each graph indicate the predicted *d*-to-*d* excitation energies of each of the Ni centers (Ni1 in red, Ni2 in green, Ni3 in blue).

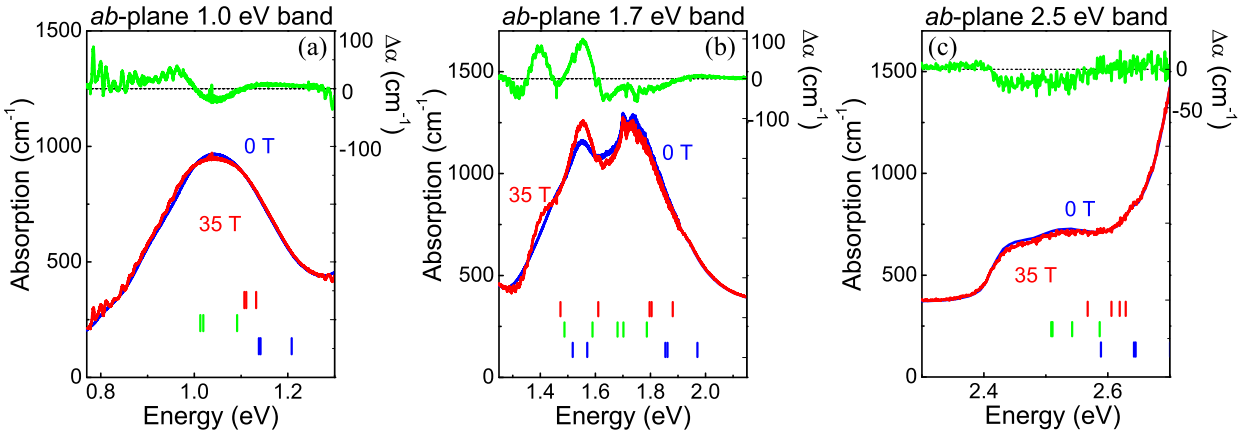

FIG. S5: Close-up views of the Ni *d*-to-*d* excitations in the vicinity of the (a) 1.0, (b) 1.7, and (c) 2.5 eV bands in the *ab*-plane. The set of vertical tick marks show the calculated excitations for each type of Ni center (Ni1 in red, Ni2 in green, Ni3 in blue). As discussed here and in the main text, the relative position of these excitations reveals the relative size of the crystal field splitting.

we know (based upon the predicted sequence of excitations) that the *d*-to-*d* excitations emanating from the Ni3 centers always govern the shape of the band tail, we surmise that the local structure around the Ni3 centers is not very sensitive to magnetic field. This is probably because the Ni3 site is already strongly distorted, allowing this metal center and the ligands around it to remain rigid under applied field. These findings are in excellent agreement with the predictions of Wu *et al.* on the importance of superexchange within the Ni1···Ni2 pair to the magnetic properties [S1].

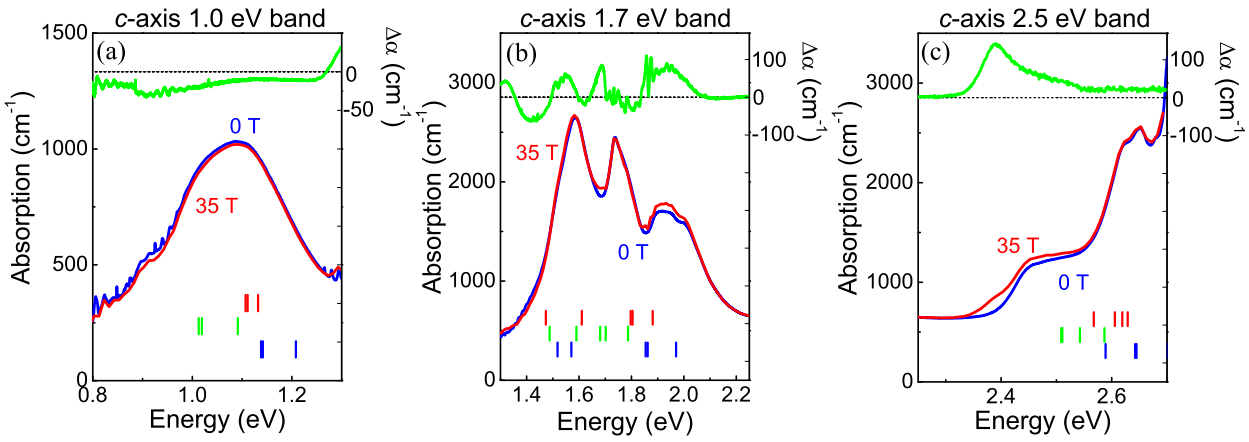

FIG. S6: Close-up views of the Ni d-to-d excitations in the vicinity of the (a) 1.0, (b) 1.7, and (c) 2.5 eV bands in the c-direction. The set of vertical tick marks at the bottom of each panel indicate the calculated excitations for each type of Ni center (Ni1 in red, Ni2 in green, Ni3 in blue) [S2].

Trends in the integrated absorption difference

The fundamental electronic excitations of Ni_3TeO_6 display a number of different trends across the 9 T spin flop transition. These are best seen in the absorption difference, $\Delta\alpha(E,B) = \alpha(E,B) - \alpha(E,B=0)$, which eliminates spectral commonalities. In a complex spectrum, it is challenging to fully disentangle energy, linewidth, and oscillator strength trends. Ni3TeO$_6$ is even worse than usual because there are three different Ni centers. This means that the band centered at 1.0 eV has 9 different oscillators! And the bands centered near 1.7 eV have a total of 15 underlying d-to-d excitations - each with their own oscillator parameters! So while we examined the lineshapes carefully to see whether specific energy, linewidth, and oscillator strength trends could be unraveled, there are no unambiguous trends. We therefore elected to employ an integral of the absolute value of the absorption difference $\int(\Delta\alpha)\mathrm{d}E$ over an appropriate energy window to track what is actually a combination of energy, linewidth, and oscillator strength changes for 9 or 15 individual oscillators. Examples of these trends, which are responsive to the static structural environment, are shown in Fig. S7. Sharp changes are observed across the spin flop transition, irrespective of the energy window in which the magneto-optical properties are analyzed. That said, oscillator strength changes can increase or decrease and even (in the case of the response centered around 1.4 eV) give an indication of the higher field transitions to come. These interesting differences may contain clues to the complex interplay of competing interactions in this material.

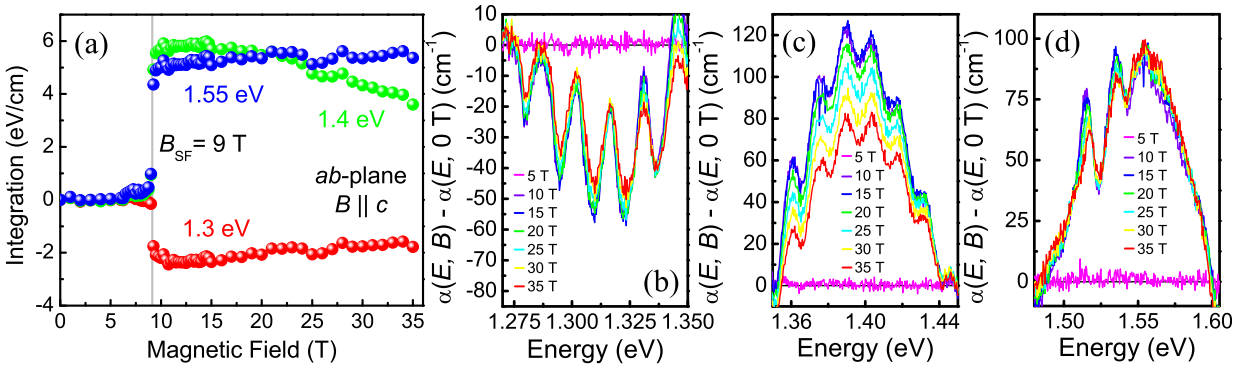

FIG. S7: (a) Integrated absorption difference vs. magnetic field in several different energy windows in the *ab*-plane. The red points correspond to analysis of the spectral data in panel (b), the green points with (c), and the blue with data in (d). The 9 T spin-flop transition is indicated by a vertical gray line.

[S1] F. Wu, E. Kan, C. Tian, and M. -H. Whangbo, Inorg. Chem. **49**, 7545 (2010).

[S2] Additional resolution is required to track changes in the exciton and phonon sidebands in applied field.